

ADSORPTION OF PRIMARY SUBSTITUTED HYDROCARBONS ONTO SOLID  
GALLIUM SUBSTRATES

by

CHRISHANI MAHESHWARI DE SILVA

B.S., Institute of Chemistry Ceylon, Sri Lanka, 2008  
Post graduate diploma in Analytical Chemistry, University of Colombo, Sri Lanka, 2011

A THESIS

Submitted in partial fulfillment of the requirements for the degree

MASTER OF SCIENCE

Department of Chemistry  
College of Art and Science

KANSAS STATE UNIVERSITY  
Manhattan, Kansas

2013

Approved by:

Major Professor  
Takashi Ito

# **Copyright**

CHRISHANI MAHESHWARI DE SILVA

2013

## Abstract

Adsorption of a series of primarily substituted hydrocarbons (RX; C<sub>18</sub>H<sub>37</sub>PO(OH)<sub>2</sub> (ODPA), C<sub>17</sub>H<sub>35</sub>COOH, C<sub>18</sub>H<sub>37</sub>OH, C<sub>18</sub>H<sub>37</sub>NH<sub>2</sub> and C<sub>18</sub>H<sub>37</sub>SH) onto solid gallium substrates with and without UV/ozone treatment was studied using contact angle goniometry, spectroscopic ellipsometry and cyclic voltammetry (CV). UV/ozone treatment offered a hydrophilic surface (water contact angle ( $\theta^{\text{water}}$ ) less than 10°), reflecting the formation of a surface oxide layer with the maximum thickness of *ca.* 1 nm and possibly the removal of surface contaminants. Upon immersion in a toluene solution of a RX,  $\theta^{\text{water}}$  increased due to adsorption of the RX onto gallium substrates. In particular, UV/ozone-treated gallium substrates (UV-Ga) immersed in an ODPA solution exhibited  $\theta^{\text{water}}$  close to 105°. The ellipsometric thickness of the adsorbed ODPA layer was *ca.* 2.4 nm and CV data measured in an acetonitrile solution showed significant inhibition of redox reaction on the substrate surface. These results indicate the formation of a densely-packed ODPA monolayer on UV-Ga. The coverage of a C<sub>17</sub>H<sub>35</sub>COOH layer adsorbed onto UV-Ga was lower, as shown by smaller  $\theta^{\text{water}}$  (*ca.* 99°), smaller ellipsometric thickness (*ca.* 1.3 nm) and smaller electrode reaction inhibition. Adsorption of the other RX onto UV-Ga was weaker, as indicated by smaller  $\theta^{\text{water}}$  (82-92°). ODPA did not strongly adsorb onto UV-untreated gallium substrates, suggesting that the ODPA adsorption mainly originates from hydrogen bond interaction of a phosphonate group with surface oxide. These results will provide a means for controlling the surface properties of oxide-coated gallium that play an essential role in monolayer conductivity measurements and electroanalytical applications.

All the results have been published as “Chrishani M De Silva, Bipin Pandey, Feng Li and Takashi Ito, Langmuir, DOI: 10.1021/la400334n

## Table of Contents

List of Figures .....	vi
List of Tables .....	viii
Dedication .....	ix
Acknowledgements .....	x
Chapter 1 - Introduction .....	1
Chapter 2 - Experimental section .....	4
2.1 Chemical and Materials .....	4
2.2 Fabrication of solid gallium films on planar gold coated silicon substrate .....	4
2.3 Surface Treatment of Solid Gallium Substrates .....	5
2.4 Instrumentation .....	6
2.4.1 Contact angle goniometry .....	6
2.4.2 Atomic force microscopy .....	7
2.4.3 Spectroscopic Ellipsometry .....	8
2.4.4 Cyclic voltammetry .....	9
Chapter 3 - Results and Discussion .....	10
3.1 UV/ozone Treatment of Solid Gallium Substrates .....	10
3.2 Adsorption of Primary Substituted Hydrocarbons on Solid Gallium Substrates .....	16
3.3 Electrochemical Characterization of Solid Gallium Surfaces .....	19
Chapter 4 - Conclusion .....	24
References .....	25

## List of Figures

Figure 1. Fabrication of solid gallium film on planer gold coated silicon substrates and UV/ozone treatment .....	4
Figure 2. A photograph of contact angle goniometry ( <a href="http://www.ptli.com/testlopedia/subs/pocket_goniometer.asp">http://www.ptli.com/testlopedia/subs/pocket_goniometer.asp</a> ).....	6
Figure 3. A photograph of atomic force microscope ( <a href="http://nano.mtu.edu/afm.htm">http://nano.mtu.edu/afm.htm</a> ).....	7
Figure 4. A photograph of spectroscopic ellipsometry instrument ( <a href="http://www3.ntu.edu.sg/home/FANHJ/Facilities.html">http://www3.ntu.edu.sg/home/FANHJ/Facilities.html</a> ).....	8
Figure 5. Experimental set up for electrochemical measurements .....	9
Figure 6. AFM images ( $\Delta z = 15$ nm) of (a) an untreated gallium substrate, (b) a UV/O <sub>3</sub> -treated gallium substrate (UV-Ga) and (c) an ODPA-coated UV-Ga. The root mean square (RMS) roughness obtained from multiple different images is (a) $0.87 \pm 0.39$ nm ( $n = 4$ ), (b) $0.74 \pm 0.17$ nm ( $n = 6$ ) and (c) $0.93 \pm 0.18$ nm ( $n = 3$ ), which is close to that of the surface of a plastic Petri dish ( $0.87 \pm 0.30$ nm ( $n = 3$ ); Figure 7), taken by Feng.Li .....	11
Figure 7. AFM image ( $\Delta z = 15$ nm) of the surface of a plastic Petri dish employed to prepare metallic gallium substrates. The root mean square (RMS) roughness obtained from three different areas is $0.87 \pm 0.30$ nm, taken by Feng Li .....	12
Figure 8 Typical ellipsometric spectra measured at a solid gallium substrate (top) just after its preparation under Ar atmosphere (untreated Ga), (middle) after UV/ozone treatment for 50 min (UV-Ga) and (bottom) after immersion in a toluene solution of ODPA for 24 hours (ODPA/UV-Ga). The dotted lines represent the fitted lines based on the layered model: A B-Spline model for an untreated Ga substrate; One Cauchy (oxide) layer on the Ga substrate for UV-Ga; An additional Cauchy layer (an organic layer) on the oxide-coated Ga substrate (UV-Ga) for ODPA/UV-Ga. For the fitting, the parameter A in the Cauchy model is fixed, and the layer thickness, the parameters B and C were varied to obtain the best fitting. The parameters (layer thickness, B and C) that gave the best fit for each spectrum are shown, in addition to the mean-square error of the fitting (MSE). Data collected by. Dr Takashi Ito	13
Figure 9 Water contact angle (blue triangles) and ellipsometric thickness of a surface oxide layer (red circles) on a solid gallium surface as a function of total UV/ozone treatment time.	

Measured on three different samples. The error bars represent the standard deviations of the data. Data collected by Dr. Takashi Ito, Chrishani M De Silva, Shinabu Ito, Bipin Pandey 15

Figure 10. Optical images of ODPA/UV-Ga (ca. 1 x 1 cm<sup>2</sup>) before (upper) and after (bottom) the solid gallium are melted at 35 °C. Note that the ODPA/UV-Ga prior to the heating has a uniform mirror-like surface taken by Chrishani M De Silva ..... 19

Figure 11. Water contact angles of an ODPA/UV-Ga substrate as a function of immersion time in water at room temperature. This data indicates that the desorption of ODPA from the UV-Ga surface is negligible in the timescale of the contact angle measurements (< 1 min). Data collected by Chrishani M. De Silva..... 20

Figure 12. CVs (scan rate: 0.1 V/s) measured in 0.1 M TBAPF<sub>6</sub>/acetonitrile at 0 °C under Ar atmosphere. (a) An untreated gallium substrate (red), a UV/O<sub>3</sub>-treated gallium substrate (UV-Ga; black) and an untreated gallium substrate upon adsorption of ODPA (blue); (b) UV/O<sub>3</sub>-treated gallium substrates (UV-Ga) with no organic layer (black; Note that this CV is the same as that shown in Figure 3a), upon adsorption of ODPA (ODPA/UV-Ga; red), C<sub>17</sub>H<sub>35</sub>COOH (C<sub>17</sub>H<sub>35</sub>COOH/UV-Ga; blue) and C<sub>18</sub>H<sub>37</sub>NH<sub>2</sub> (C<sub>18</sub>H<sub>37</sub>NH<sub>2</sub>/UV-Ga; green). Data collected by Chrishani M. De Silva ..... 21

## List of Tables

Table 1. Cauchy Model Parameters (Average $\pm$ Standard Deviation) Obtained from Multiple Ellipsometric Spectra. ....	14
Table 2. Water Contact Angles ( $\theta^{\text{water}}$ ) of Chemically Modified Ga Substrates and Ellipsometric Thicknesses of Adsorbed Organic Layers .....	17
Table 3. Anodic and Cathodic Voltage Limits for Gallium Substrates with and without Surface Oxide and Adsorbed Organic Layers.....	22

## **Dedication**

This work is dedicated to my parents.

## **Acknowledgements**

I would like to thank my research advisor, Prof. Takashi Ito for all the help and consideration during my graduate study. I would also like to thank the members of the Ito group that I had the privilege of working with Mr. Bipin Pandey, Mr. Feng Li ,Mr. Hoa TranBa and Ms. Shinabu Ito. Also, I want to thank my committee members, Prof Daniel Higgins and Prof. Keith Hohn for their time and feedback. I am particularly grateful to Ms. Earline Dikeman for providing care and numerous help during my life here and Mr. Martin Courtois for all his help during thesis preparation. I would like to give my greatest gratitude to my husband, Rishard Packee, my parents and my elder brother. They have given me solid support and great love and encouragements during all the time. I would like to thank the Chemistry Department of Kansas State University for giving me a unique opportunity to study here, and Division of Chemical Sciences, Geosciences and Biosciences, Office of Basic Energy Sciences of the U.S. Department of Energy for financial support for this work. And finally I would like to thank all my friends who are not listed here for their enormous support.

## Chapter 1 - Introduction

Gallium is a non-toxic, non-volatile liquid metal (m.p. 29.8 °C; b.p 2477K) discovered by French chemist Paul Emile Lecoq de Boisbaudran in 1875. The molecular weight of gallium is 69.72 and natural gallium can exist as a mixture of two stable isotopes  $Ga_{69}$  and  $Ga_{71}$ .<sup>1</sup> Gallium can form a non-metallic, thin film of self-passivating semiconducting oxide layer ( $Ga_2O_3$ , ~1nm) on gallium surface upon exposure to the air and also can maintain oxide free conditions using standard ultra high vacuum conditions.<sup>3</sup> Gallium can form three oxides such as  $Ga_2O$ ,  $GaO$  and  $Ga_2O_3$ . The most common and stable oxide is  $Ga_2O_3$  and can exist in five types ( $\alpha$ ,  $\beta$ ,  $\gamma$ ,  $\delta$ ,  $\epsilon$ ). The crystal structure of  $Ga_2O_3$  is corundum type and it is similar to aluminum oxide. The chemical properties of gallium metal is different from aluminum as it has lower melting point, softness and the ability to be reduced to lower oxidation compounds.<sup>1</sup>

Gallium and its alloys have recently attracted considerable interest as electrode materials because of their low melting point and low toxicity. For example, Galanstain (eutectic mixture of gallium, indium and tin) electrode material shows comparable behavior to mercury in voltametric analysis of cadmium and lead. Galanstain has a higher hydrogen over potential, higher potential window and its renewable surface led to give higher reproducibility of results as mercury electrode does.<sup>2</sup> Gallium film electrode has been proposed to eliminate copper interference on zinc determination in anodic stripping voltammetry.<sup>3</sup> These findings shows that we can take an advantage of gallium and its alloy electrodes as alternative to toxic mercury for trace metal ion analysis in voltammetry. Eutectic gallium indium (EGaIn) is a another alloy of gallium metal. It can be easily incorporated into  $\mu\text{m}$ -scale channels, leading to fabrication of

microelectrodes within microfluidic channels.<sup>4-6</sup> Another advantage of EGaIn is it is an elastic material and can be molded at room temperature<sup>3</sup>. And also EGaIn is electrically conductive thus can be used as a contact electrodes for measurements of electrical conductivity across self-assembled monolayers (SAMs) formed on another metal surfaces.<sup>5, 8-10</sup> Solid metallic gallium can form self organized nanoporous anodic oxide monoliths in the presence of 4 and 6M H<sub>2</sub>SO<sub>4</sub> at 10 and 15V. These monoliths pore diameters are ranging from 18-40 nm and can be used for future chemical sensors and catalyst applications.<sup>7</sup>

In these applications, it is important to understand the surface chemistry of these metals. It is well-known that metallic gallium is self-passivated by an ultrathin gallium oxide layer ( $\leq 1$  nm thick) upon exposure to air.<sup>4, 11</sup> The oxide layer gives significant influences on electrochemical and conductivity measurements, including passivation of electron conduction and direct involvement in the redox reactions of a gallium electrode.<sup>4, 12, 13</sup> In addition, chemisorption onto gallium electrodes will provide a means for modulating the electrical and electrochemical properties of gallium/alloy electrodes, as has been shown for other electrode materials in chemically modified electrodes.<sup>14</sup> However, the surface chemistry of metallic gallium has attracted limited attention. X-ray reflectivity method<sup>11</sup> and Auger electron spectroscopy<sup>4</sup> were used to measure surface oxide formation on metallic gallium and its alloys. Electrochemical methods exhibited the adsorption of ionic species onto gallium electrodes in aqueous solutions.<sup>12</sup> Interestingly, it is known that the surface oxide layers of gallium alloys consist of mainly gallium oxide due to the very high reactivity of gallium with oxygen as compared to the other metallic components.<sup>4</sup> Thus, it is important to understand the chemical properties of surface gallium oxide layers for the aforementioned applications.

In this study, adsorption of organic molecules on solid metallic gallium was systematically investigated using contact angle goniometry, spectroscopic ellipsometry, atomic force microscopy (AFM) and cyclic voltammetry (CV). The effects of UV/ozone treatment on surface properties of a solid gallium surface were also investigated. As organic molecules, primary substituted hydrocarbons (RX) with long alkyl chains and different terminal functional groups (-X = -PO(OH)<sub>2</sub>, -COOH, -OH, -NH<sub>2</sub> and -SH) were examined. Their long alkyl chains facilitate the assessment of molecular adsorption, which can be recognized as an increase in water contact angle ( $\theta^{\text{water}}$ ) and ellipsometric thickness<sup>15</sup> as well as the passivation of electrode reactions.<sup>16</sup> Considering that surface oxide layers formed on liquid gallium and its alloys have solid-like properties,<sup>4, 11</sup> knowledge obtained in this study will provide a guidance to select an organic functional group suitable for SAM conductivity measurements and surface functionalization of a gallium electrode in electrochemical applications.

## Chapter 2 - Experimental section

### 2.1 Chemical and Materials

High purity gallium (99.99%) was purchased from GalliumSource, LLC and used as received. Gold-coated silicon substrates, which were prepared by sputtering 10 nm of titanium followed by 200 nm of gold onto Si(100) wafers, were purchased from LGA Thin Films (Foster City, CA). n-Octadecylphosphonic acid ( $C_{18}H_{37}PO(OH)_2$ ; Alfa Aesar), n-octadecanoic acid ( $C_{17}H_{35}COOH$ ; Aldrich), n-octadecanol ( $C_{18}H_{37}OH$ ; Alfa Aesar), n-octadecylamine ( $C_{18}H_{37}NH_2$ ; Alfa Aesar), n-octadecyl mercaptan ( $C_{18}H_{37}SH$ ; Acros Organics), tetrabutylammonium hexafluorophosphate ( $TBAPF_6$ ; Strem Chemicals), and anhydrous acetonitrile (Alfa Aesar) were used as received. Toluene (Fisher Scientific) was dried over activated molecular sieves 3A (Acros Organics) prior to use.

### 2.2 Fabrication of solid gallium films on planar gold coated silicon substrate

The surface of planar Au substrate (6mm X 6mm ) was cleaned in a Novascan PSD-UVT UV-ozone system for 45 minutes. A drop of liquid gallium spread over cleaned Au substrate. The gallium coated Au substrate was positioned on a sterile polystyrene Petri dish and freeze samples upside down on a Petri dish (Figure 01. steps 1,2,3 ). Detached the gallium coated Au substrates from Petri dish and obtained mirror like shinny gallium films.

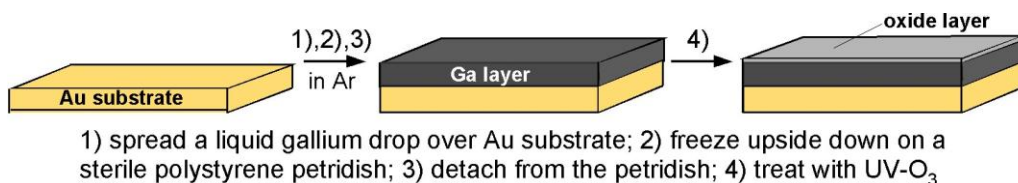


**Figure 1. Fabrication of solid gallium film on planer gold coated silicon substrates and UV/ozone treatment**

### **2.3 Surface Treatment of Solid Gallium Substrates**

UV/ozone treatment (Figure 1, step 4) of the resulting solid gallium substrates were carried out using a Novascan PSD-UVT UV-ozone system (ca. 20 mW/cm<sup>2</sup>). To prevent a gallium film from melting, the sample stage of the instrument needed to be cooled with an ice pack every 10 minutes of UV/ozone treatment. Solid gallium substrates were immersed in 5 mM toluene solutions of RX for 24 hours, washed thoroughly with toluene and dried under an Ar stream. Adsorption of RX was completed after 24-hours immersion according to water contact angle measurements.<sup>17</sup>

## 2.4 Instrumentation

### 2.4.1 Contact angle goniometry

Contact angle goniometry measures the contact angle through the liquid where liquid/vapor interface meets a solid surface. This can be used to measure static contact angle, advancing and receding contact angles. Water contact angle data can use to demonstrate surface wettability and Young's equation can be used to measure surface energy of a system.<sup>27</sup> Water contact angles on solid gallium samples were measured using a PG-1 pocket contact angle goniometer for the two sides of a water drop (2  $\mu\text{L}$ ) within 30 s after deposition of the drop.<sup>17, 18</sup>

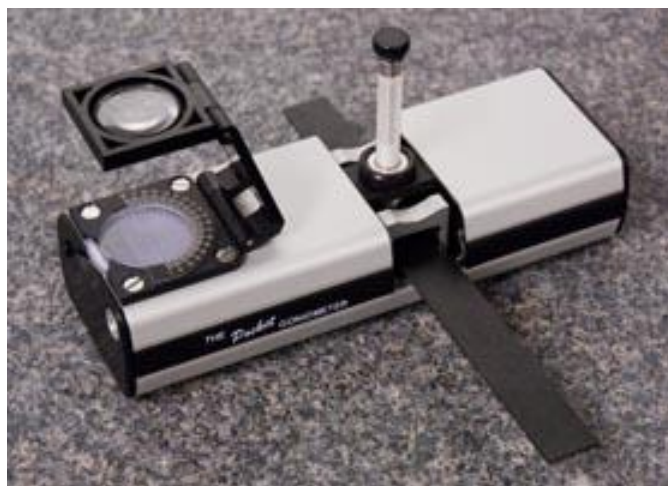


**Figure 2. A photograph of contact angle goniometry**  
([http://www.ptli.com/testlopedia/subs/pocket\\_goniometer.asp](http://www.ptli.com/testlopedia/subs/pocket_goniometer.asp))

### ***2.4.2 Atomic force microscopy***

AFM operation modes can be divided into two main types, contact mode and non contact mode depending on where cantilever is vibrated. In this study AFM images were obtained by contact-mode imaging in air using a Digital Instrument Multimode AFM with Nanoscope IIIa electronics. Contact mode tips from Vista Probes were employed.

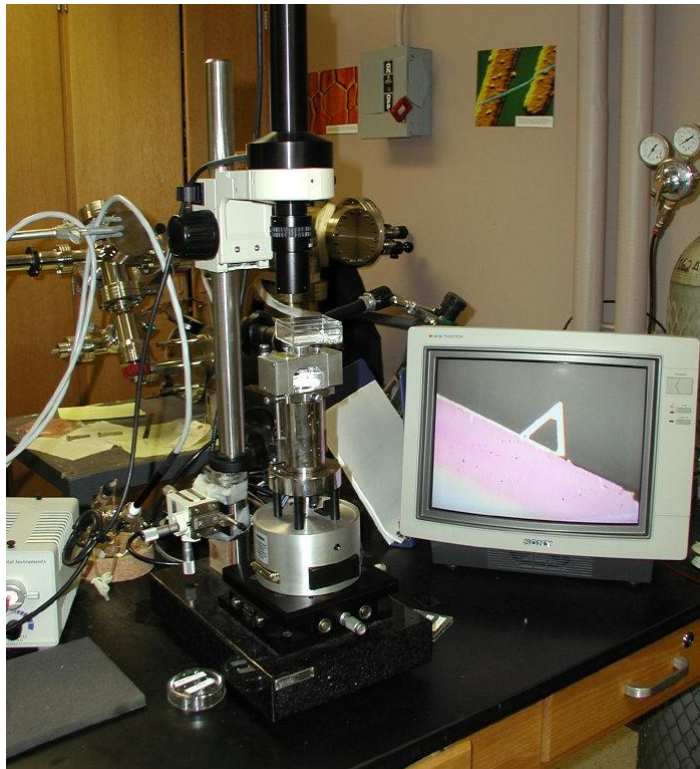


**Figure 3. A photograph of atomic force microscope (<http://nano.mtu.edu/afm.htm>)**

### 2.4.3 Spectroscopic Ellipsometry

Spectroscopic ellipsometry is an optical technique and it has been used to characterize thin film thickness, optical constant of multilayer and nonuniform gradient. The basic operation principle is based on change of polarization light in reflection or transmission. In this experiment spectroscopic ellipsometry measurements were performed using a J.A. Woollam Alpha SE spectroscopic ellipsometer. A series of ellipsometric spectra on each gallium substrate were recorded before and after UV/ozone treatment and upon subsequent RX adsorption as follows.<sup>17</sup> An ellipsometric spectrum of a freshly-prepared gallium substrate prior to UV/ozone treatment (untreated Ga) was first recorded, and was used as a spectrum of an underlying substrate. Then, a spectrum was recorded for the same substrate after UV/ozone treatment (UV-Ga) to obtain the thickness of a surface oxide layer. Finally, a spectrum of the substrate upon immersion in a RX solution was recorded to determine the thickness of an adsorbed organic layer.



**Figure 4. A photograph of spectroscopic ellipsometry instrument ( <http://www3.ntu.edu.sg/home/FANHJ/Facilities.html> )**

#### 2.4.4 Cyclic voltammetry

CV measurements were carried out in a three-electrode cell containing a silver quasi-reference electrode (AgQRE; ca. -0.68 V vs.  $\text{Fc}/\text{Fc}^+$ ) and a platinum counter electrode inside a glove bag continuously flowing Ar. A gallium substrate was immobilized at the bottom of the electrochemical cell with the geometric electrode area defined by an O-ring (8 mm in diameter) as reported previously.<sup>7</sup> All the CV data were obtained in 0.1 M TBAPF<sub>6</sub> acetonitrile solution cooled by ice (ca. 0 °C) using a CH instruments model 618B electrochemical analyzer. All the CV data shown were recorded at the first potential cycle. Very similar voltammograms were measured also at the second cycle.

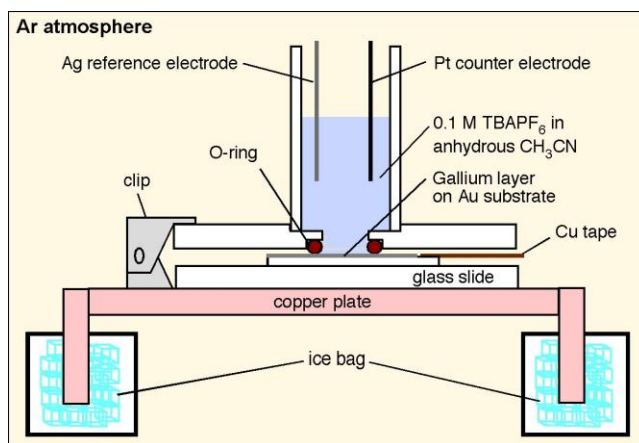


**Figure 5. Experimental set up for electrochemical measurements**

## Chapter 3 - Results and Discussion

In this study, the effects of UV/ozone treatment on the surface properties of solid metallic gallium were first investigated using AFM, contact angle goniometry and spectroscopic ellipsometry. Subsequently, adsorption of the different RX onto solid gallium substrates with and without UV/ozone treatment (UV-Ga and untreated Ga, respectively) was studied using the three techniques. Finally, the electrochemical properties of the solid gallium substrates with and without surface oxide and adsorbed organic layers were measured using CV in an acetonitrile solution. These experiments revealed the chemical properties of the solid gallium surfaces, and also the affinity of the terminal functional groups of RX to these surfaces.

### 3.1 UV/ozone Treatment of Solid Gallium Substrates

Figure 6ab shows AFM images of a solid gallium substrate before and after UV/ozone treatment. Overall, the surfaces are fairly smooth, as indicated by their root-mean-square (RMS) roughness of less than 1 nm. The surface features probably reflect those of a plastic Petri dish that was used for the preparation of the solid gallium substrate. Indeed, the RMS roughness of untreated Ga ( $0.87 \pm 0.39$  nm; Figure 6a) is very similar to that of the plastic Petri dish ( $0.87 \pm 0.30$  nm; Figure 7). Very similar surface features were also measured by us with scanning electron microscopy.<sup>7</sup> Importantly, there is no significant change in surface morphology upon UV/ozone treatment, as indicated by the similar RMS roughness ( $0.74 \pm 0.17$  nm; Figure 6b). Thus, the experimental procedure based on layered models (vide supra) is applicable to analyze ellipsometric spectra for estimation of surface layer thickness.

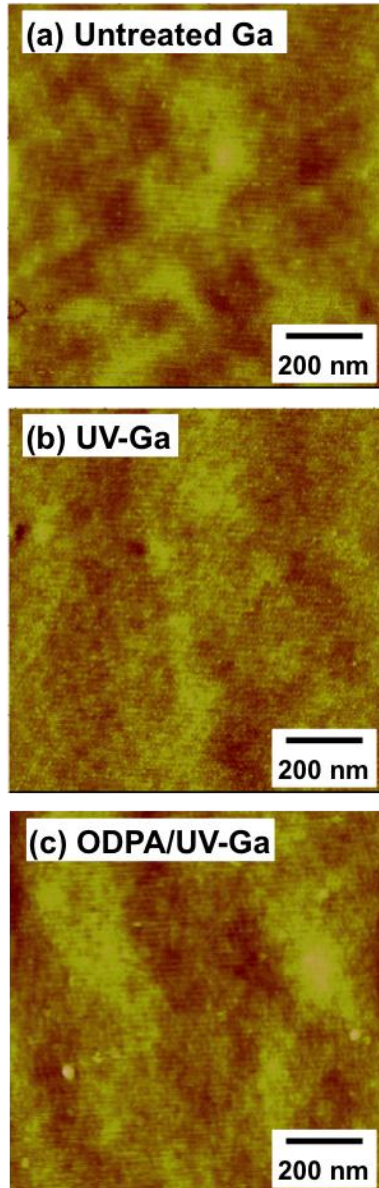


**Figure 6.** AFM images ( $\Delta z = 15$  nm) of (a) an untreated gallium substrate, (b) a UV/O<sub>3</sub>-treated gallium substrate (UV-Ga) and (c) an ODPA-coated UV-Ga. The root mean square (RMS) roughness obtained from multiple different images is (a)  $0.87 \pm 0.39$  nm ( $n = 4$ ), (b)  $0.74 \pm 0.17$  nm ( $n = 6$ ) and (c)  $0.93 \pm 0.18$  nm ( $n = 3$ ), which is close to that of the surface of a plastic Petri dish ( $0.87 \pm 0.30$  nm ( $n = 3$ ); Figure 7), taken by Feng.Li

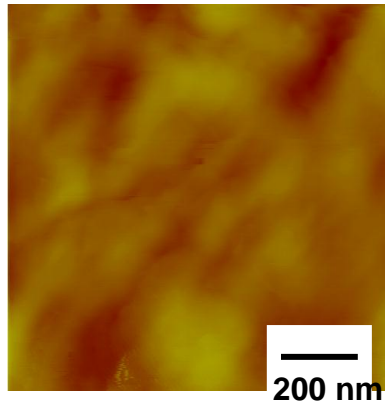
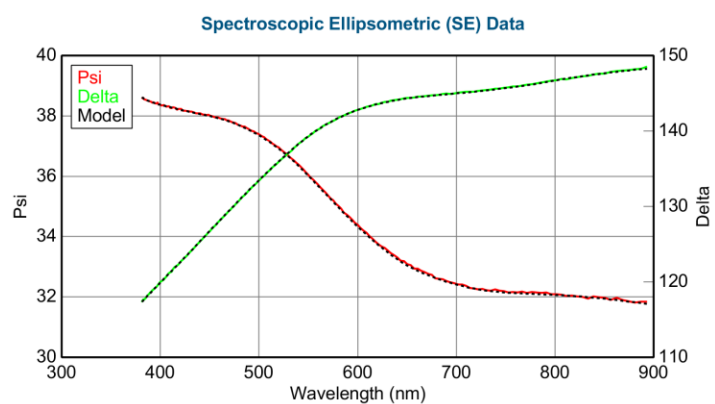
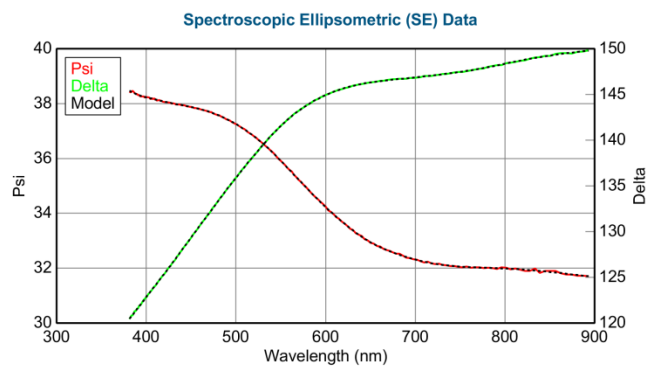
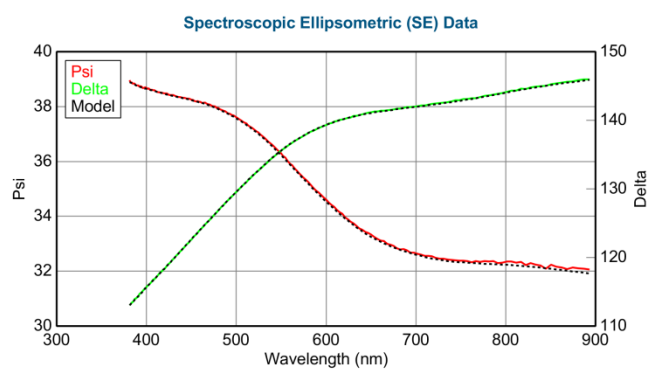


**Figure 7. AFM image ( $\Delta z = 15$  nm) of the surface of a plastic Petri dish employed to prepare metallic gallium substrates. The root mean square (RMS) roughness obtained from three different areas is  $0.87 \pm 0.30$  nm, taken by Feng Li**

A series of typical ellipsometric spectra obtained from one gallium substrate are shown in Figure 8. Reliable data could be obtained only when a series of data were measured at almost the same area. A spectrum for an untreated Ga was fitted using a B-spline model. The thickness of surface oxide and adsorbed organic layers were determined by adding Cauchy layers on top of the B-spline model. For the fitting, the parameter  $A$  in the Cauchy model ( $n = A + B/\lambda^2 + C/\lambda^4$ ;  $n$  is the refractive index and  $\lambda$  ( $\mu\text{m}$ ) is the wavelength) was fixed:  $A = 1.89^{19}$  for an oxide layer and  $A = 1.45^{20}$  for an additional organic layer. The average  $B$  and  $C$  parameters as well as the layer thicknesses obtained from spectroscopic ellipsometry measurements are summarized in Table 01.



MSE = 0.821  
 Thickness # 1 =  $10.71 \pm 0.127 \text{ \AA}$   
 B =  $-0.07921 \pm 0.010725$



MSE = 1.235  
 Thickness # 2 =  $21.69 \pm 0.366 \text{ \AA}$   
 B =  $0.03045 \pm 0.008257$

**Figure 8** Typical ellipsometric spectra measured at a solid gallium substrate (top) just after its preparation under Ar atmosphere (untreated Ga), (middle) after UV/ozone treatment for 50 min (UV-Ga) and (bottom) after immersion in a toluene solution of ODPa for 24 hours (ODPa/UV-Ga). The dotted lines represent the fitted lines based on the layered model: A B-Spline model for an untreated Ga substrate; One Cauchy (oxide) layer on the Ga substrate for UV-Ga; An additional Cauchy layer (an organic layer) on the oxide-coated Ga substrate (UV-Ga) for ODPa/UV-Ga. For the fitting, the parameter A in the Cauchy model is fixed, and the layer thickness, the parameters B and C were varied to obtain the best fitting. The parameters (layer thickness, B and C) that gave the best fit for each spectrum are shown, in addition to the mean-square error of the fitting (MSE). Data collected by. Dr Takashi Ito

**Table 1. Cauchy Model Parameters (Average  $\pm$  Standard Deviation) Obtained from Multiple Ellipsometric Spectra.**

Sample	# of data	Thickness (nm)	<i>B</i>	<i>C</i>
10 min UV-treated	8	0.63 $\pm$ 0.29	0.14 $\pm$ 0.72	-0.018 $\pm$ 0.090
20 min UV-treated	8	0.85 $\pm$ 0.22	0.09 $\pm$ 0.47	-0.010 $\pm$ 0.058
30 min UV-treated	8	0.98 $\pm$ 0.33	0.04 $\pm$ 0.42	-0.004 $\pm$ 0.051
40 min UV-treated	8	1.00 $\pm$ 0.32	0.04 $\pm$ 0.34	-0.003 $\pm$ 0.042
50 min UV-treated	8	1.09 $\pm$ 0.31	-0.10 $\pm$ 0.08	-0.014 $\pm$ 0.007
ODPA/UV-Ga	6	2.4 $\pm$ 0.4	0.028 $\pm$ 0.051	-0.0037 $\pm$ 0.0061
C <sub>17</sub> H <sub>35</sub> COOH/UV-Ga	7	1.3 $\pm$ 0.4	0.121 $\pm$ 0.126	-0.0125 $\pm$ 0.0131
C <sub>18</sub> H <sub>37</sub> NH <sub>2</sub> /UV-Ga	3	1.1 $\pm$ 0.5	0.336 $\pm$ 0.263	-0.0390 $\pm$ 0.0339

<sup>a</sup> Average  $\pm$  standard deviation of data measured for three different samples. The anodic and cathodic limits were defined as the potentials where a Faradaic current was larger than 0.25  $\mu$ A ( $\Delta j = 0.5 \mu$ A/cm<sup>2</sup>) at the scan rate of 0.1 V/s. The Faradaic current was determined by subtracting a background current (e.g., a charging current). <sup>b</sup>

Calculated from a difference between the anodic and cathodic limits of each substrate. Data collected by Dr. Takashi Ito, Chrishani M De Silva, Shinabu Ito, Bipin Pandey

Figure 9 shows the water contact angles ( $\theta^{\text{water}}$ ) and ellipsometric thicknesses of surface layers on solid gallium substrates as a function of total UV/ozone treatment time. Upon UV/ozone treatment, the surfaces changed to be hydrophilic ( $\theta^{\text{water}} < 10^\circ$ ), and the ellipsometric thickness of surface oxide layers increased up to *ca.* 1 nm. The very limited oxide growth was previously reported as the passivation of metallic gallium and its alloys.<sup>4, 11</sup> The higher hydrophilicity probably reflects the formation of an oxide layer as well as the removal of surface contaminants. Although the  $\theta^{\text{water}}$  values for solid gallium samples upon 10-50 min UV/ozone treatment were  $< 10^\circ$  in the figure, it could be recognized that water spread easily on substrates upon UV/ozone treatment for longer than 30 min. Thus, gallium substrates were treated by UV/ozone for 50 min in total to prepare UV-Ga thereafter.

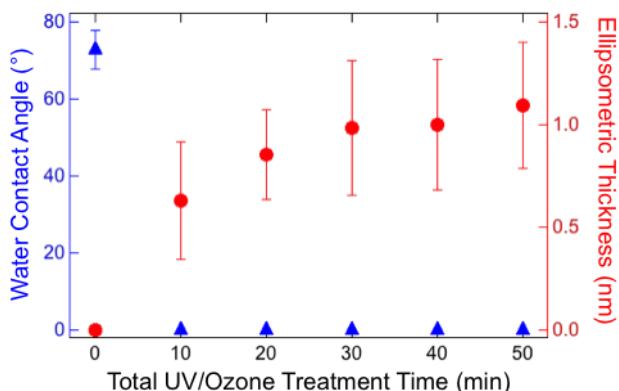


**Figure 9** Water contact angle (blue triangles) and ellipsometric thickness of a surface oxide layer (red circles) on a solid gallium surface as a function of total UV/ozone treatment time. Measured on three different samples. The error bars represent the standard deviations of the data. Data collected by Dr. Takashi Ito, Chrishani M De Silva, Shinabu Ito, Bipin Pandey

### 3.2 Adsorption of Primary Substituted Hydrocarbons on Solid Gallium Substrates

Table 2 summarizes the  $\theta^{\text{water}}$  values of untreated Ga and UV-Ga before and after their immersion in toluene solutions with and without RX for 24 hours. The  $\theta^{\text{water}}$  values upon immersion in RX solutions were significantly larger than those upon immersion in toluene, reflecting the adsorption of RX onto the substrates. Overall, UV-Ga offered larger increases in  $\theta^{\text{water}}$  than untreated Ga. In particular, the very large  $\theta^{\text{water}}$  value for ODPA-adsorbed UV-Ga ( $\theta^{\text{water}} \approx 105^\circ$ ) suggests the formation of a densely-packed monolayer, as reported on other metal oxide surfaces.<sup>21</sup> In contrast, adsorption of RX onto untreated Ga was weak, as indicated by the smaller increases in  $\theta^{\text{water}}$ . The  $\theta^{\text{water}}$  values of RX-adsorbed UV-Ga are in the order of  $\text{C}_{18}\text{H}_{37}\text{PO}(\text{OH})_2 > \text{C}_{17}\text{H}_{35}\text{COOH} > \text{C}_{18}\text{H}_{37}\text{OH} > \text{C}_{18}\text{H}_{37}\text{NH}_2 > \text{C}_{18}\text{H}_{37}\text{SH}$ . This order corresponds to that of hydrogen bond acidity of the functional groups,<sup>22</sup> indicating the significance of the hydrogen bond accepting properties (*i.e.*, basicity) of the surface gallium oxide on the adsorption of RX. The stronger adsorption of ODPA may also reflect the heterocondensation of the phosphonic acid moiety with the surface oxide layer, as reported for other metal oxide surfaces.<sup>21</sup> The difference in adsorption strength was further verified by spectroscopic ellipsometry and CV (*vide infra*). It should be noted that only  $\text{C}_{18}\text{H}_{37}\text{NH}_2$  was examined for the spectroscopic ellipsometry and CV measurements among the three RX that showed weaker adsorption onto UV-Ga (*i.e.*,  $\text{C}_{18}\text{H}_{37}\text{NH}_2$ ,  $\text{C}_{18}\text{H}_{37}\text{SH}$  and  $\text{C}_{18}\text{H}_{37}\text{OH}$ ).

**Table 2. Water Contact Angles ( $\theta^{\text{water}}$ ) of Chemically Modified Ga Substrates and Ellipsometric Thicknesses of Adsorbed Organic Layers**

	$\theta^{\text{water}}$ on untreated Ga ( $^{\circ}$ ) <sup>a</sup>	$\theta^{\text{water}}$ on UV-Ga ( $^{\circ}$ ) <sup>a,b</sup>	Ellipsometric Thickness (nm) <sup>a</sup>
No immersion in a solution	73 ± 5 [22]	< 10	
Immersion in toluene	66 ± 11 [30]	52 ± 14 [30]	
C <sub>18</sub> H <sub>37</sub> SH <sup>c</sup>	87 ± 1 [4]	82 ± 4 [8]	- <sup>d</sup>
C <sub>18</sub> H <sub>37</sub> NH <sub>2</sub> <sup>c</sup>	88 ± 2 [4]	85 ± 5 [12]	1.1 ± 0.5 [3]
C <sub>18</sub> H <sub>37</sub> OH <sup>c</sup>	90 ± 2 [4]	92 ± 3 [8]	- <sup>d</sup>
C <sub>17</sub> H <sub>35</sub> COOH <sup>c</sup>	94 ± 2 [4]	99 ± 6 [17]	1.3 ± 0.4 [7]
C <sub>18</sub> H <sub>37</sub> PO(OH) <sub>2</sub> (ODPA) <sup>c</sup>	93 ± 2 [4]	105 ± 4 [24]	2.4 ± 0.4 [6]

<sup>a</sup> Average ± standard deviation. The numbers of measurements are shown in square brackets. <sup>b</sup> Gallium substrates treated with UV/ozone for 50 minutes in total. <sup>c</sup> Gallium substrates were immersed in a toluene solution (5 mM) for 24 hours. <sup>d</sup> Not measured. Data collected by Chrishani M De Silva, Dr. Takashi Ito, Shinabu Ito

Figure 6c shows an AFM image of an ODPA-coated UV-Ga. The surface roughness and features were very similar to those on untreated Ga and UV-Ga (Figure 6ab), as indicated by the very similar RMS roughness ( $0.93 \pm 0.18$  nm). This observation suggests the formation of a very thin and uniform monolayer upon immersion in an ODPA solution. Organosilane SAMs may also be formed on UV-Ga as with other metal oxides, but may offer less uniform surfaces due to the formation of thick, polymeric layers.<sup>15</sup> Table 2 also shows the ellipsometric thicknesses of ODPA, C<sub>17</sub>H<sub>35</sub>COOH and C<sub>18</sub>H<sub>37</sub>NH<sub>2</sub> layers adsorbed onto UV-Ga. The ellipsometric thickness of an ODPA layer ( $2.4 \pm 0.4$  nm) was close to the length of a C18 alkyl chain in all-trans configuration,<sup>20</sup> supporting the formation of a densely-packed monolayer as anticipated from the large  $\theta_{\text{water}}$  values. In contrast, the other two RX gave smaller ellipsometric thicknesses, suggesting that the adsorbed layers were packed more loosely. It should be pointed out that the stability of the ODPA SAMs upon conversion from solid to liquid gallium could not be assessed using contact angle and ellipsometric measurements because of the significant change in surface morphology (Figure 10). Thus, heating-induced heterocondensation, which has been often employed for organophosphonate SAMs on other metal oxides,<sup>21</sup> cannot be employed to improve the stability of ODPA SAMs on gallium.



**Figure 10. Optical images of ODPA/UV-Ga (ca. 1 x 1 cm<sup>2</sup>) before (upper) and after (bottom) the solid gallium are melted at 35 °C. Note that the ODPA/UV-Ga prior to the heating has a uniform mirror-like surface taken by Chrishani M De Silva**

### **3.3 Electrochemical Characterization of Solid Gallium Surfaces**

Electrochemical methods provide a simple means for investigating the properties of passivation layers formed on conductor surfaces.<sup>16, 23</sup> In this study, CV was employed to assess the passivation properties of surface oxide and/or adsorbed organic layers at solid gallium substrates. CV measurements were carried out in an acetonitrile solution containing 0.1 M TBAPF<sub>6</sub>, because the adsorbed organic layers gradually desorbed from solid gallium substrates in an aqueous solution (Figure 11) as observed on GaN and AlGa<sub>0.5</sub>N substrates for ODPA monolayers.<sup>17, 18, 24</sup> The surface oxide and adsorbed organic layers were assessed based on anodic and cathodic voltage limit (electrochemical potential window) obtained from CV data.

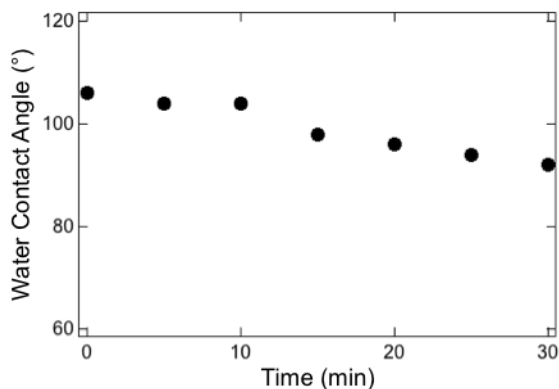


**Figure 11. Water contact angles of an ODPA/UV-Ga substrate as a function of immersion time in water at room temperature. This data indicates that the desorption of ODPA from the UV-Ga surface is negligible in the timescale of the contact angle measurements (< 1 min). Data collected by Chrishani M. De Silva**

Figure 12a shows cyclic voltammograms measured at untreated Ga, UV-Ga and ODPA-modified untreated Ga (ODPA/Ga) in 0.1 M TBAPF<sub>6</sub>/acetonitrile. The anodic and cathodic currents in these voltammograms possibly originate from the oxidation and reduction of a trace amount of water in the acetonitrile solution as well as the formation and reduction of a surface oxide layer. Untreated Ga exhibited the narrowest electrochemical potential window due to the absence of a passivation layer. UV-Ga showed the inhibition of anodic and cathodic reactions to give wider electrochemical potential window, suggesting that a surface oxide layer inhibited the electrode reactions. An ODPA layer adsorbed on untreated Ga inhibited cathodic reactions. However, the electrochemical potential window of ODPA/Ga was much narrower than that of ODPA/UV-Ga (see Figure 12b) probably due to the low ODPA coverage as suggested by the smaller  $\theta^{\text{water}}$  (Table 2; vide supra).

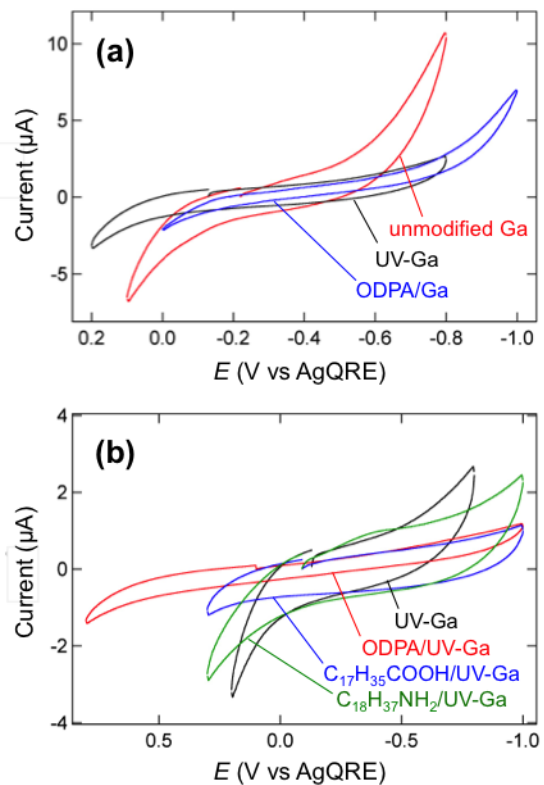


**Figure 12. CVs (scan rate: 0.1 V/s) measured in 0.1 M TBAPF6/acetonitrile at 0 °C under Ar atmosphere. (a) An untreated gallium substrate (red), a UV/O<sub>3</sub>-treated gallium substrate (UV-Ga; black) and an untreated gallium substrate upon adsorption of ODPA (blue); (b) UV/O<sub>3</sub>-treated gallium substrates (UV-Ga) with no organic layer (black; Note that this CV is the same as that shown in Figure 3a), upon adsorption of ODPA (ODPA/UV-Ga; red), C<sub>17</sub>H<sub>35</sub>COOH (C<sub>17</sub>H<sub>35</sub>COOH/UV-Ga; blue) and C<sub>18</sub>H<sub>37</sub>NH<sub>2</sub> (C<sub>18</sub>H<sub>37</sub>NH<sub>2</sub>/UV-Ga; green). Data collected by Chrishani M. De Silva**

Figure 12b shows cyclic voltammograms measured at UV-Ga modified with ODPA (ODPA/UV-Ga), C<sub>17</sub>H<sub>35</sub>COOH (C<sub>17</sub>H<sub>35</sub>COOH/UV-Ga) and C<sub>18</sub>H<sub>37</sub>NH<sub>2</sub> (C<sub>18</sub>H<sub>37</sub>NH<sub>2</sub>/UV-Ga), in addition to a cyclic voltammogram at UV-Ga shown in Figure 12a. ODPA/UV-Ga offered the widest electrochemical potential window, indicating that the adsorbed ODPA inhibited the electrode reactions most efficiently. The small charging current also supports the high coverage of the electrode surface with ODPA. In contrast, the voltammogram at C<sub>18</sub>H<sub>37</sub>NH<sub>2</sub>/UV-Ga was similar to that at UV-Ga due to the weak adsorption of C<sub>18</sub>H<sub>37</sub>NH<sub>2</sub> to UV-Ga, as shown by the smaller  $\theta^{\text{water}}$  value and ellipsometric thickness

**Table 3. Anodic and Cathodic Voltage Limits for Gallium Substrates with and without Surface Oxide and Adsorbed Organic Layers**

Ga substrates	Anodic limit (V) <sup>a</sup>	Cathodic limit (V) <sup>a</sup>	$\Delta E_{\text{window}}$ (V) <sup>b</sup>
	Untreated Ga		
UV/O <sub>3</sub> -treated Ga (UV-Ga)	0.054 ± 0.060	-0.592 ± 0.037	0.646 ± 0.059
Untreated Ga with ODPA (ODPA/Ga)	-0.072 ± 0.141	-0.692 ± 0.017	0.620 ± 0.124
ODPA/UV-Ga	0.657 ± 0.006	-0.902 ± 0.032	1.559 ± 0.038
C <sub>17</sub> H <sub>35</sub> COOH/UV-Ga	0.259 ± 0.061	-0.895 ± 0.149	1.153 ± 0.098
C <sub>18</sub> H <sub>37</sub> NH <sub>2</sub> /UV-Ga	0.055 ± 0.059	-0.618 ± 0.124	0.673 ± 0.076

<sup>a</sup> Average ± standard deviation of data measured for three different samples. The anodic and cathodic limits were defined as the potentials where a Faradaic current was larger than 0.25 μA ( $\Delta j = 0.5 \mu\text{A}/\text{cm}^2$ ) at the scan rate of 0.1 V/s. The Faradaic current was determined by subtracting a background current (e.g., a charging current). <sup>b</sup> Calculated from a difference between the anodic and cathodic limits of each substrate. Data collected by Chrishani M. De Silva

Table 3 summarizes the anodic/cathodic voltage limits and electrochemical potential window ( $\Delta E_{\text{window}}$ ) determined from the voltammograms at the solid gallium substrates examined. The anodic and cathodic voltage limits are defined as the potentials where a Faradaic current is larger than a threshold value. Previously, linear sweep voltammetry was employed to determine the voltage limits based on various threshold currents under different scan rates.<sup>25, 26</sup> Here, the limit is defined as a potential where a Faradaic current obtained as a result of the subtraction of a background current is larger than  $0.25 \mu\text{A}$  ( $0.5 \mu\text{A}/\text{cm}^2$ ) in voltammograms measured at the scan rate of  $0.1 \text{ V/s}$ . The background subtraction eliminates the influence of a charging current and an Ohmic resistance.

The  $\Delta E_{\text{window}}$  values in Table 3 confirm that electrochemical potential window is wider in the order of untreated Ga < ODPA/Ga  $\sim$  UV-Ga  $\sim$  C<sub>18</sub>H<sub>37</sub>NH<sub>2</sub>/UV-Ga < C<sub>17</sub>H<sub>35</sub>COOH/UV-Ga < ODPA/UV-Ga. In particular, there is a good correlation between  $\theta_{\text{water}}$ , ellipsometric thickness and  $\Delta E_{\text{window}}$  for the three UV-Ga samples with adsorbed organic layers: ODPA formed a densely-packed monolayer on UV-Ga to give the large  $\theta_{\text{water}}$ , ellipsometric thickness corresponding to the molecular length, and the most efficient passivation shown by the wide  $\Delta E_{\text{window}}$ . The adsorption of C<sub>17</sub>H<sub>35</sub>COOH onto UV-Ga was weaker than ODPA, giving smaller  $\theta_{\text{water}}$ , smaller ellipsometric thickness and narrower  $\Delta E_{\text{window}}$ . C<sub>18</sub>H<sub>37</sub>NH<sub>2</sub> did not strongly adsorb onto UV-Ga, leading to negligible passivation upon its adsorption onto the substrate. These electrochemical results verify the high affinity of a functional group with higher hydrogen bond acidity onto a surface gallium oxide layer on solid metallic gallium.

## Chapter 4 - Conclusion

In this work, we investigated the adsorption of primary substituted hydrocarbons on solid gallium substrates with and without UV/ozone treatment. UV/ozone treatment gave hydrophilic surfaces with surface oxide layers up to 1 nm in thickness. Adsorption of primary hydrocarbons onto UV-O<sub>3</sub> substrates were driven by the hydrogen bonding acidity of organic functional groups. According to the measured contact angle data we can hypothesis that gallium oxide shows basic oxide properties. The surface oxide layer shows extremely lower water contact angle  $\ll 10$  throughout the 50 minutes time intervals. Based on these results we can claim that formed surface oxide layer is higher hydrophilic in nature and it may show smooth surface characteristics. Further surface roughness data of AFM images are supporting to this claim. However adsorptions onto UV-O<sub>3</sub> non treated gallium substrates were comparatively poor as pure metallic gallium surface may not exhibit basic surface properties. The findings of this work elaborate that ODPA formed a densely-packed monolayer on UV-O<sub>3</sub> treated gallium substrate. Results from contact angle measurements, ellipsometric thickness and efficient electrode passivation provide evidence that ODPA formed well packed monolayer. Although other organic functional groups did not show strong adsorption onto UV-O<sub>3</sub> substrates except -COOH. This observation is consistence with hydrogen bond acidity of organic functional groups. In contrast, any of organic functional groups were not showed strong adsorption onto UV-O<sub>3</sub> non treated gallium substrates. It indicates that gallium oxide layer has a significant influence on adsorption process. These results will provide guidance to the control of electron transfer/conduction across gallium-organic layer interfaces and also to controlled functionalization of gallium, its alloys and their oxide surfaces.

## References

1. N. Israelachvili, J., *Intermolecular and Surface Forces*. Academic press: San Diego, CA, 1991
2. Surmann, P.; Zeyat, H. Voltammetric Analysis Using a Self-Renewable Non-Mercury Electrode. *Anal. Bioanal. Chem.* **2005**, *383*, 1009-1013.
3. Tyszczyk, K.; Korolczuk, M.; Grabarczyk, M. Application of Gallium Film Electrode for Elimination of Copper Interference in Anodic Stripping Voltammetry of Zinc. *Talanta* **2007**, *71*, 2098-2101.
4. Dickey, M. D.; Chiechi, R. C.; Larsen, R. J.; Weiss, E. A.; Weitz, D. A.; Whitesides, G. M. Eutectic Gallium-Indium (EGaIn): A Liquid Metal Alloy for the Formation of Stable Structures in Microchannels at Room Temperature. *Adv. Funct. Mater.* **2008**, *18*, 1097-1104.
5. Nijhuis, C. A.; Reus, W. F.; Barber, J. R.; Dickey, M. D.; Whitesides, G. M. Charge Transport and Rectification in Arrays of SAM-Based Tunneling Junctions. *Nano Lett.* **2010**, *10*, 3611-3619.
6. So, J.-H.; Dickey, M. D. Inherently Aligned Microfluidic Electrodes Composed of Liquid Metal. *Lab Chip* **2011**, *11*, 905-911.
7. Pandey, B.; Thapa, P. S.; Higgins, D. A.; Ito, T. Formation of Self-Organized Nanoporous Anodic Oxide from Metallic Gallium. *Langmuir* **2012**, *28*, 13705-13711.
8. Chiechi, R. C.; Weiss, E. A.; Dickey, M. D.; Whitesides, G. M. Eutectic Gallium-Indium (EGaIn): A Moldable Liquid Metal for Electrical Characterization of Self-Assembled Monolayers. *Angew. Chem. Int. Ed.* **2008**, *47*, 142-144.
9. Fracasso, D.; Valkenier, H.; Hummelen, J. C.; Solomon, G. C.; Chiechi, R. C. Evidence for Quantum Interference in SAMs of Arylethynylene Thiolates in Tunneling Junctions with Eutectic Ga-In (EGaIn) Top-Contacts. *J. Am. Chem. Soc.* **2011**, *133*, 9556-9563.
10. Reus, W. F.; Thuo, M. M.; Shapiro, N. D.; Nijhuis, C. A.; Whitesides, G. M. The SAM, Not the Electrodes, Dominates Charge Transport in Metal-Monolayer//Ga<sub>2</sub>O<sub>3</sub>/Gallium-Indium Eutectic Junctions. *ACS Nano* **2012**, *6*, 4806-4822.
11. Regan, M. J.; Tostmann, H.; Pershan, P. S.; Magnussen, O. M.; DiMasi, E.; Ocko, B. M.; Deutsch, M. X-Ray Study of the Oxidation of Liquid-Gallium Surfaces. *Phys. Rev. B* **1997**, *55*, 10786-10790.

12. Popova, T. I.; Bagotskaya, I. A.; Moorhead, E. D. Gallium. In *Encyclopedia of Electrochemistry of the Elements, Volume 8, Ag, Mg, Ga, N, Actinides*, Bard, A. J., Ed. Marcel Dekker: New York, 1978; pp 207-262.
13. Wade, T.; Ross, C. B.; Crooks, R. M. Electrochemical Synthesis of Ceramic Materials .5. An Electrochemical Method Suitable for the Preparation of Nine Metal Nitrides. *Chem. Mater.* **1997**, *9*, 248-254.
14. Murray, R. W.; Ewing, A. G.; Durst, R. A. Chemically Modified Electrodes - Molecular Design for Electroanalysis. *Anal. Chem.* **1987**, *59*, 379A-390A.
15. Ulman, A. *An Introduction to Ultrathin Organic Films: from Langmuir-Blodgett to Self-Assembly*. Academic Press: London, 1991.
16. Love, J. C.; Estroff, L. A.; Kriebel, J. K.; Nuzzo, R. G.; Whitesides, G. M. Self-Assembled Monolayers of Thiolates on Metals as a Form of Nanotechnology. *Chem. Rev.* **2005**, *105*, 1103-1169.
17. Ito, T.; Forman, S.; Cao, C.; Li, F.; Eddy, C.; Mastro, M.; Holm, R.; Henry, R.; Hohn, K.; Edgar, J. Self-Assembled Monolayers of Alkylphosphonic Acid on GaN Substrates. *Langmuir* **2008**, *24*, 6630-6635.
18. Li, F.; Shishkin, E.; Mastro, M.; Hite, J.; Eddy, C.; Edgar, J.; Ito, T. Photopolymerization of Self-Assembled Monolayers of Diacetylenic Alkylphosphonic Acids on Group-III Nitride Substrates. *Langmuir* **2010**, *26*, 10725-10730.
19. Rebien, M.; Henrion, W.; Hong, M.; Mannaerts, J.; Fleischer, M. Optical Properties of Gallium Oxide Thin Films. *Appl. Phys. Lett.* **2002**, *81*, 250-252.
20. Bain, C. D.; Troughton, E. B.; Tao, Y. T.; Evall, J.; Whitesides, G. M.; Nuzzo, R. G. Formation of Monolayer Films by the Spontaneous Assembly of Organic Thiols from Solution onto Gold. *J. Am. Chem. Soc.* **1989**, *111*, 321-335.
21. Hotchkiss, P. J.; Jones, S. C.; Paniagua, S. A.; Sharma, A.; Kippelen, B.; Armstrong, N. R.; Marder, S. R. The Modification of Indium Tin Oxide with Phosphonic Acids: Mechanism of Binding, Tuning of Surface Properties, and Potential for Use in Organic Electronic Applications. *Acc. Chem. Res.* **2012**, *45*, 337-346.
22. Abraham, M. H.; Platts, J. A. Hydrogen Bond Structural Group Constants. *J. Org. Chem.* **2001**, *66*, 3484-3491.

23. Bard, A. J.; Faulkner, L. R. *Electrochemical Methods, Fundamentals and Applications*. Second Edition ed.; Wiley: New York, 2001.
24. Kim, H.; Colavita, P.; Paoprasert, P.; Gopalan, P.; Kuech, T.; Hamers, R. Grafting of Molecular Layers to Oxidized Gallium Nitride Surfaces via Phosphonic Acid Linkages. *Surf. Sci.* **2008**, *602*, 2382-2388.
25. Morita, M.; Goto, M.; Matsuda, Y. Ethylene Carbonate-Based Organic Electrolytes for Electric Double-Layer Capacitors. *J. Appl. Electrochem.* **1992**, *22*, 901-908.
26. Xu, K.; Ding, S. P.; Jow, T. R. Toward Reliable Values of Electrochemical Stability Limits for Electrolytes. *J. Electrochem. Soc.* **1999**, *146*, 4172-4178.